EVALUATION OF A GAS-LIQUID STIRRED REACTOR EMULATOR VIA NETWORK MODELS

Nor Aishah Saidina Amin Department of Chemical Engineering Universiti Teknologi Malaysia Kuala Lumpur
and
R. MANN Department of Chemical Engineering University of Manchester Inst of Science and Technology Manchester England

Abstract

Backmixed stirred reactor has always been the first choice equipment for carrying out gas-liquid reactions. However, they may not be the best, mainly because of the non-uniform gas distribution in the vessel. Moreover, the gas-liquid flow behaviour is not clearly understood partly due to the complex interactions between gas and liquid. Due to these reasons, a model which can first predict the internal behaviour of the two-phase flow accurately is needed. A 2-D experimental rig has been used to study the gas-liquid flow behaviour. From photographic evaluations, valuable insight of the gas-liquid flow in the vessel is obtained. Two models have been tested to evaluate the experimental results. The models are able to predict the local gas hold-up, which is an important variable to predict the gas-liquid flow pattern. The first model is the simple zones-in-loops based on the gas and liquid flowing in loops through a series of eight backmixed zones in the half 2-D stirred vessel. The second model is a more complex equal sized square cells network which accommodates a more realistic liquid flow pattern and thus, a more successful prediction of the two-phase flow behaviour. The predicted local gas hold-ups are exhibited on a unique 3-D spatial map. They display very encouraging predictive values in comparison with the experimental results. With improvements in the bubble detection techniques and also by assuming non-uniform bubble size the model has a potential to predict accurately not only the hydrodynamics characteristics, but also the physico-chemical interactions.

1.0 Introduction

Reactions involving gas and liquid such as halogenations, fermentations and hydrogenations are common in industries. One example is the liquid phase hydrocarbon oxidation where many reactions are often involved. Typical schemes are shown here:

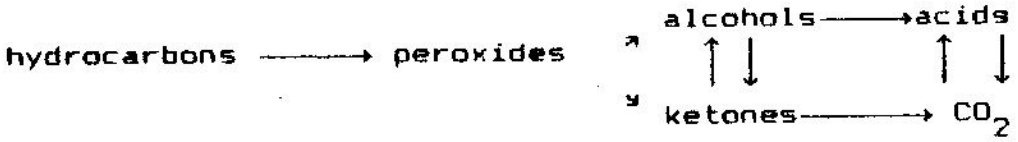

Gas-liquid reactions are mostly carried out in backmixed stirred reactors because they are suitable for almost all reactions, and also, being simple are more economical. However, the reactor could behave non-ideally and thus the assumption of no spatial variations in gas and liquid concentration could lead to a wrong reactor design. The most common correlations available to calculate important design parameters such as the average gas hold-up, $\bar{\varepsilon}_g$, and the volumetric mass transfer coefficient, $k_l a$ are very empirical which make them inappropriate for reaction engineering calculations. Therefore, it is important to obtain a correct picture on the internal behaviour of gas and liquid mixing and also on the mass transfer rates before reaching a more superior reactor configuration.

Complex reactions such as the one shown above produce many by-products with different qualities. The quality is related to the selectivity toward desired products, and the by-products can reduce the selectivity. In order to control the selectivity, the interplay between gas and liquid mixing and the mass transfer in stirred vessels must be studied through a more fundamental approach.

This work investigates the internal gas-liquid flow behaviour in a stirred vessel with air and water as the system. The experimental rig represents the two dimensional version of a half-tank stirred vessel with disk turbine impeller. Two theories will be used to analyze the two phase flows. The first theory is based on a simple zones-in-loops model(Mann,1981). The gas and liquid is picturized to flow in circulation loops through a series of 2x2 backmixed zones in the upper and lower half of the vessel. The second theory is based on a more complex analysis of the gas and liquid flow pattern. The model envisages the vessel as 2(10 x 10) equal sized squares meant to behave like 200 small backmixed vessels. The square cells network model (Mann and Hackett,1988) is able to accommodate flexible liquid flow patterns in a network of cells and to calculate the circulation,

disengagement and flow of the gas for any mode of injection.

Gas hold-ups have a strong influence on the performance of reactors because the gas residence time, interfacial area and the design volume of a reactor depend on them. The experimental local gas hold-ups will be compared qualitatively with the predicted results. From these results the gas-liquid flow behaviour in a stirred vessel will be more clearly understood.

2.0 Experimental

Several experiments with different air and water flow rates were carried out to obtain the overall and local gas hold-ups. An experimental rig was constructed from two glazing panes about 118.0 cm wide, 176.0 cm high and 2.8 cm apart. The narrow space between these panes made it appear like a two dimensional tank. A schematic diagram is shown in Fig.1. The circulatory agitation effects which simulated the radial flows generated by a disk turbine were provided by pumping tap water in and out of the vessel in a closed loop via two connected copper pipes about 1.1 cm O.D and 90.0 cm high. These pipes were immersed into the left-hand side of the vessel. One of the copper pipings was bent into an 'L' shape to terminate at a position equivalent to the tip of a disk turbine impeller. The other pipe had small holes at the end of it to withdraw air-water into the output line. The holes were covered with fine wire gauze to discourage air bubbles from being sucked by the pump. The 'impeller' was located mid-way of the liquid height. Air was introduced to the vessel through a sparger unit located at 10.5 cm below the tip of the 'impeller'. The 'L'-shape air sparger was made from a 1 m glass tubing with a nozzle attached to its end. Both water and air flow rates were controlled by rotameters, and the corresponding values in m^3/s were given by the calibration charts. The air rotameter was a tube size 7 with float type K while the water rotameter was a tube size 47 with float type S. A centrifugal pump was used to pump the air-water mixture.

2.1 Method

With reference to Fig.1, the experimental procedures are presented below.

Line 13 was connected to valve 2, V2, before the main pipe was turned on. Water was filled into the vessel from the main pipe through V2 and line 2 up to three-quarter of the vessel height. Then ,Line 13 was shut off followed by V2 to form a closed loop of the system. The centrifugal pump was switched on, and valve 3, V3, was opened slowly to let any residual gas in line 2 and line 5 escape through the top opening of the vessel. When the input

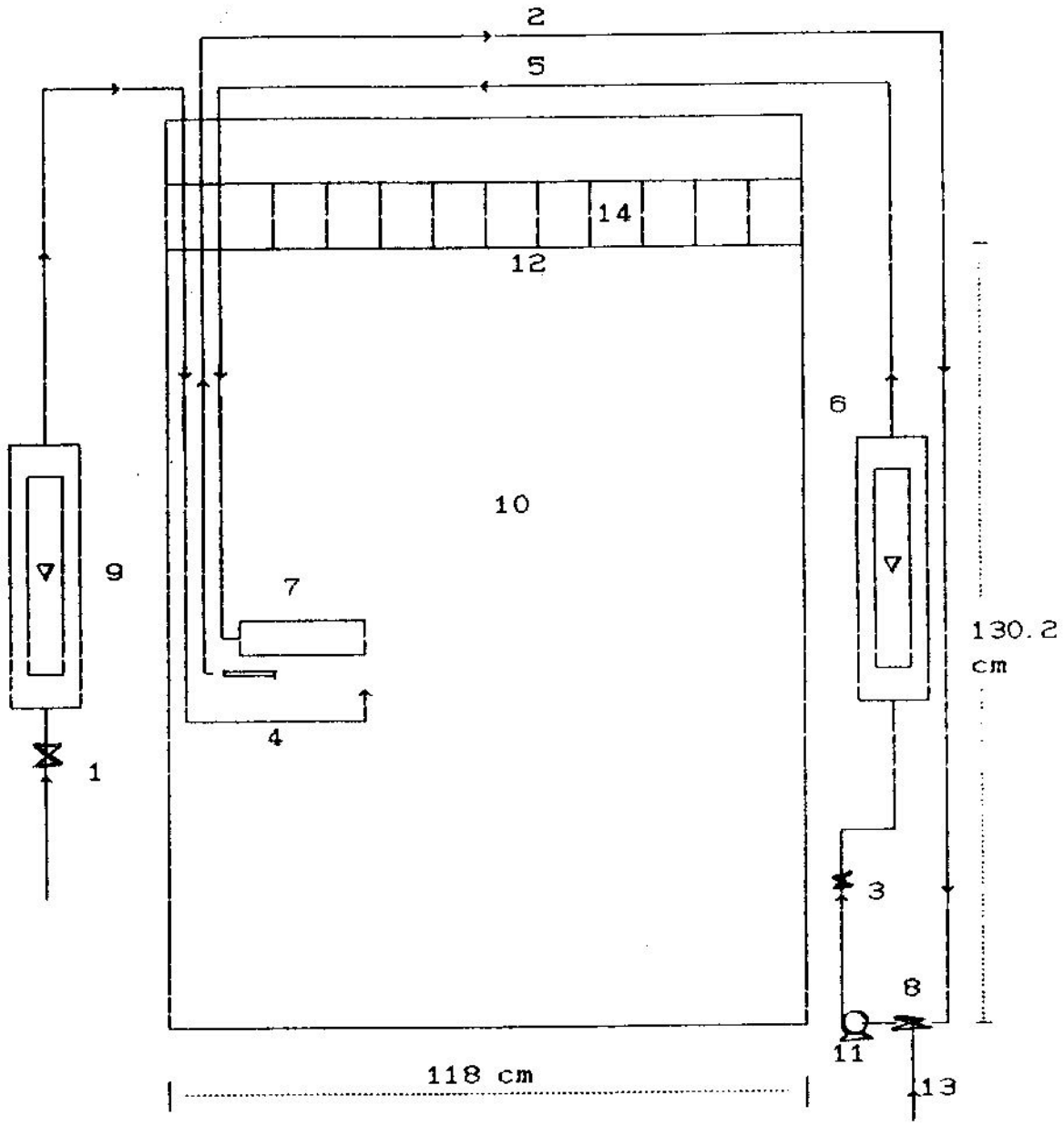

Fig 1 : Schematic diagram of the experimental rig

1. Valve 1, V1; 2. Output line; 3. Valve 3, V3; 4. Sparger

5. Input line ; 6. Liquid rotameter ; 7 'Impeller' blade

8. Valve 2, V2; 9. Air rotameter ; 10. 2-D experimental rig

11. Centifugal pump; 12. Liquid height; 13. Main pipe line

14. Marked positions to calculate water increment

line,(Line 5) and the output line,(Line 2) was free off any trapped air, the centrifugal pump was switched off. The water height was adjusted to 130.2 cm either by decreasing the level through the syphon method or simply by adding water from the top. Then, the water pumping flow rate was increased to the desired value. Keeping the water flow rate constant air was sparged in. For each air flow rate, a photograph was taken to record the gas-liquid flow pattern and to calculate the overall gas hold-up.

3.0 Overall gas hold-up calculation

The overall gas hold-up is calculated according to the procedure listed below:

1. The dynamic liquid height, H_L, for a certain water pumping flow rate without any air Qg=0.0 was photographed.

2. At a specific gas input rate air was sparged in. The dynamic liquid height under aerated conditions, H_0, was allowed to reach steady-state before it was photograped. The liquid pumping rate under a certain gas input rate, Qp, was recorded.

3. The average heights, $\bar{H}_L$ and $\bar{H}_0$, were measured at 11 different positions across the vessel. These positions were marked as No.14 in Fig.1. The overall gas hold-up, $\bar{\varepsilon}_g$ was calculated from the unaerated average dynamic liquid height, $\bar{H}_L$, and the aerated average dynamic liquid height, $\bar{H}_0$ or,

$$\bar{\varepsilon}_g = (\bar{H}_0 - \bar{H}_L) / \bar{H}_0 \qquad \text{Eqn 1}$$

4.0 Theory

The zones-in-loops model(Mann,1981) is shown in Fig 2. The gas and liquid flows pump out of the 'impeller' region into upward and downward flowing streams moving respectively into the upper and lower parts of the vessel. The model calculates the local gas hold-ups at steady-state condition by using Eqn 2.

$$u_s \approx u_t = \frac{u_G}{\varepsilon_i(0)} \pm \frac{u_L}{1-\varepsilon_i(0)} \qquad \text{Eqn.2}$$

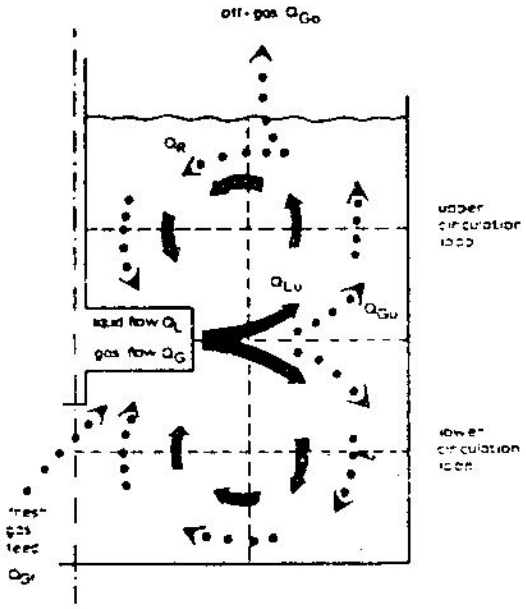

Fig 2: The Zones - in - loops model.

The square-cells model (Mann and Hackett,1988) is depicted in Fig.3 with the (row,column)-(i,j) convention for identifying the individual cells indicated on it. It contains 10x20 fixed network of equal sized square cells. The local and overall gas hold-up is calculated by using the main programme called TANK (Hackett,1985). The input file consists of the liquid pumping flow rates, gas input rates, bubble rise velocity, liquid relative velocities and positions at where the gas is sparged in. The liquid velocity profile is assumed to be similar to the results of Cooper et.al's(Cooper, 1968). The liquid velocity is obtained by multiplying the velocity factor (Saidina Amin,1988) with the relative velocties. The liquid turbulence factor, is assumed to be 20% in all cases.

For comparisons between the zones-in-loops model and the square cells model a specific run at gas input volumetric flow rate of $2.72 \times 10^{-4} m^3/s$ and aerated liquid pumping rate of $9.79 \times 10^{-4} m^3/s$ is analyzed. Pic.1 exhibits the real experimental situation for this run.

5.0 Example simulation via the zones-in-loops model

Pic.1 is analyzed by the 2x2 zones in the two loops i.e four zones in the upper vessel and another four zones in the lower vessel.

The gas path in Pic.1 shows that most of the larger bubbles that are in the upper half of the vessel either leave the water surface or stay at the water surface. Only a small fraction of small bubbles are recirculated towards the impeller region. Therefore the gas recirculation ratio, γ^*,is predicted to be between 0 to 10%.

About 90% of the air, or gas split ratio $\beta^* = 0.9$ is estimated to go to the upper surface because the lower half of the vessel is almost devoid of gas. The liquid split ratio ,α^*, is predicted to be 50% because the impeller is situated midway between the liquid surface.

The local gas hold-up distributions in Fig.4(a) and Fig.4 (b) show that the model is quite successful in predicting that the local gas hold-up in a backmixed reactor cannot be uniform. Zones 2 and 4 contain the highest hold-up in the vessel. This is qualitatively true because 90% of the air enters the zone as soon as it is sparged in.

Fig.4(a) assumes that $\gamma^*=0.0$ or no gas recirculates into the left-side of the upper vessel. Therefore, the local gas hold-up in these zones, zones 1 and 3 is zero. The hold-up values are predicted higher in zones 6 and 8 than

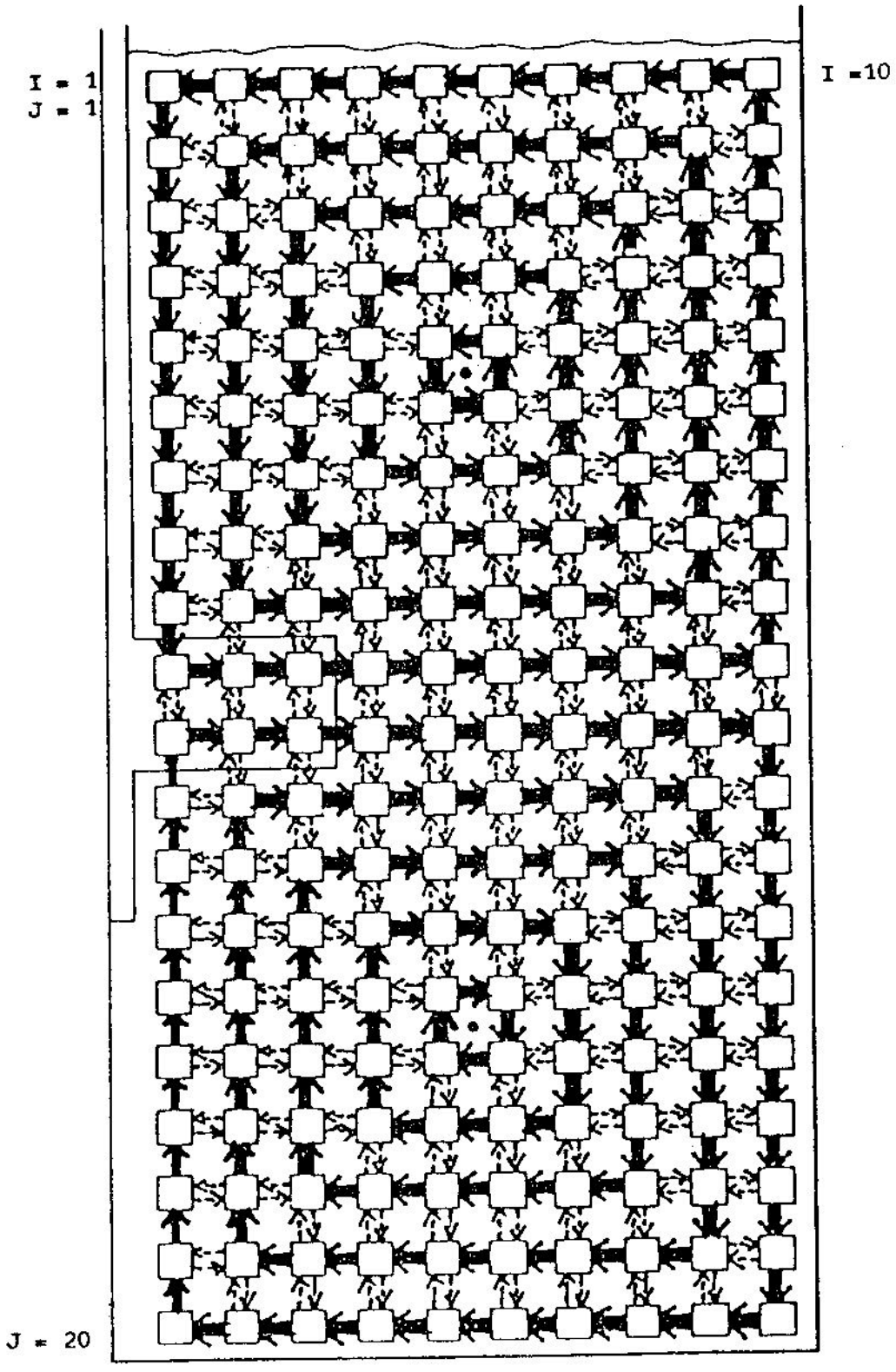

Fig 3: The Square Cells Network Model

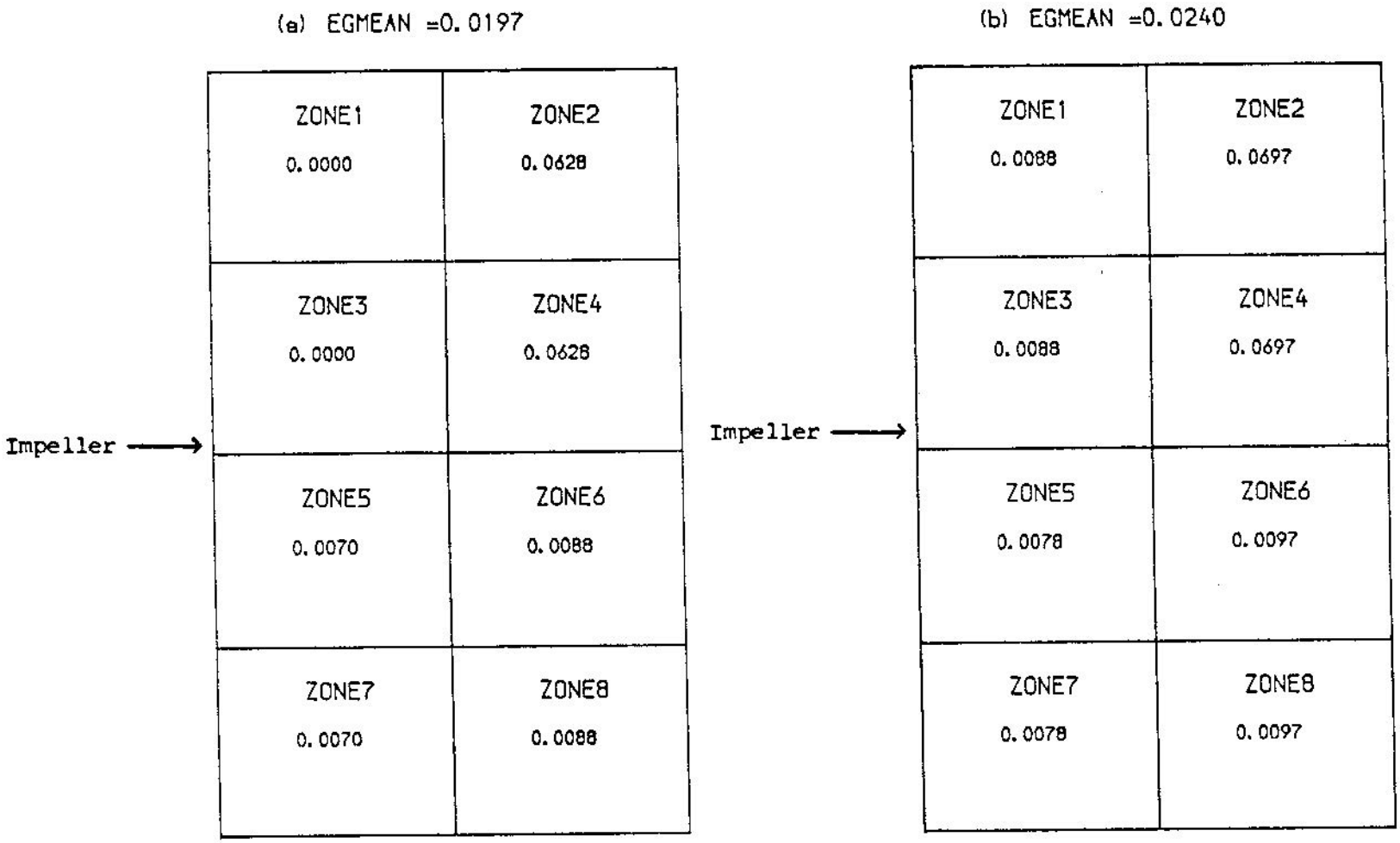

Fig 4: Local Gas Hold-up Distribution Via Zones - In - Loops Model

in zones 5 and 7 because the downward liquid direction helps to suppress the air bubbles from moving upwards.

Fig.4(b) assumes a 10% gas recirculation. Now, regions 1 and 3 show that the local gas hold-up is 0.88%. The other zones also show slight increament in the gas hold-up. Otherwise, the local gas hold-up distribution shows a similar trend to the one shown in Fig 4a. The overall gas hold-up has also increased to 2.4%. Both $\bar{\varepsilon}_g$ for conditions γ^*=0.0 and 0.1 are below the experimental value of 3.81%

The discrepancies between the predicted and experimental results may be due to the reasons below. The model divides the vessel into eight equal backmixed zones but, it actually considers four equal mixed zones only, because of the simple upward and downward water flow assumption. As a result, the model predicts the gas hold-ups in pairs, depending on the water flow directions. The model predicts some gas hold-ups in the lower vessel. In contrast, Pic.1 shows that there is only a slight patch of air bubbles in the lower vessel which are mostly concentrated to the left of zone 6. By considering only the axial directions, the model fails to consider that the bubbles have a high buoyancy force and the radial water flow helps the bubbles move freely in the vessel. The liquid flow also experience some turbulence as indicated by the water surface movement. This is why we observe, the gas hold-ups are not evenly distributed in the vessel. The discrepancy is also partly due to the uniform bubble rise velocity assumption. The model assumes that the bubble rise velocity is u_t=0.235 m/s which is the value for bubble sizes in the range of 3-8 mm. However, Pic.1 shows that there is a large variation in bubble sizes, between the region along the injected air path and elsewhere in the vessel.

Another model is therefore needed to overcome these shortcomings. The square cells network model which will be described in the next section is an improved model to this one. In this application, it contains 2(10x 10) cells of backmixed zones and predicts the flow developed by the agitator as an axisymetric two dimensional flow of liquid which is divided into 5 circulatory loops in each half of the vessel.

5.1 Example simulation via the square-cells network model

Fig.5(a) and 5(b) show the predicted local gas hold-up distributions for conditions applying to Pic.1 by the square-cells network model. The predicted overall gas hold-up value differs about 50% from the experimental value partly due to the fact that single bubble size is

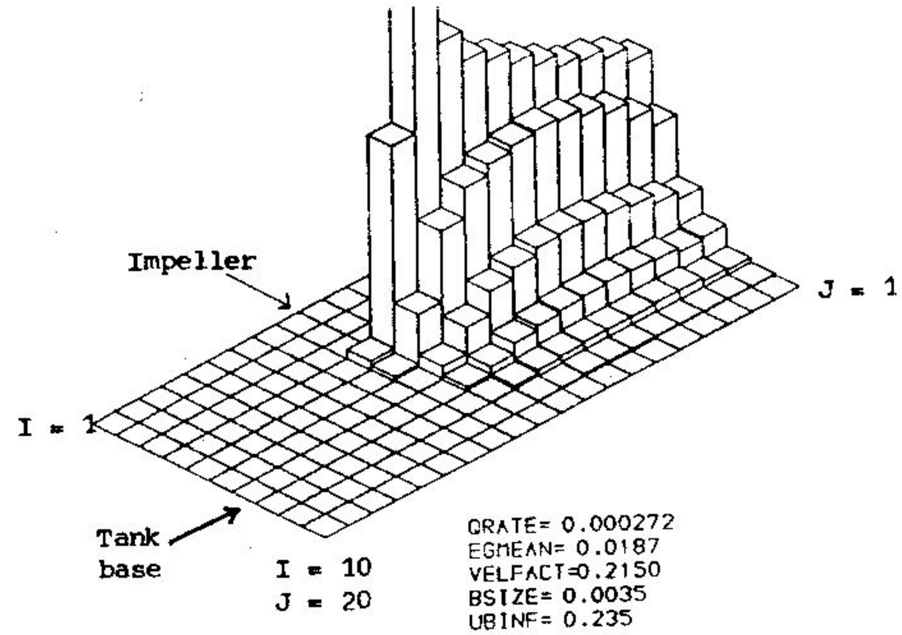

(a)

I = 1, J = 1 (top left); I = 10 (top right); Impeller → (row J = 10); J = 20 (bottom left)

0.011	0.025	0.068	0.110	0.076	0.036	0.019	0.005	0.002	0.001
0.002	0.018	0.055	0.120	0.088	0.041	0.017	0.006	0.002	0.001
0.001	0.006	0.040	0.127	0.100	0.047	0.020	0.008	0.002	0.001
0.001	0.004	0.028	0.131	0.107	0.050	0.021	0.008	0.002	0.001
0.000	0.003	0.023	0.140	0.112	0.053	0.022	0.007	0.002	0.001
0.000	0.002	0.016	0.149	0.114	0.054	0.021	0.007	0.002	0.000
0.000	0.001	0.009	0.159	0.112	0.053	0.020	0.007	0.002	0.000
0.000	0.000	0.000	0.167	0.108	0.048	0.018	0.006	0.002	0.000
0.000	0.000	0.000	0.187	0.101	0.041	0.015	0.005	0.001	0.000
0.000	0.000	0.000	0.232	0.081	0.026	0.008	0.003	0.001	0.000
0.000	0.000	0.000	0.137	0.035	0.009	0.003	0.001	0.000	0.000
0.000	0.000	0.000	0.006	0.003	0.001	0.000	0.000	0.000	0.000
0.000	0.000	0.000	0.000	0.000	0.000	0.000	0.000	0.000	0.000
0.000	0.000	0.000	0.000	0.000	0.000	0.000	0.000	0.000	0.000
0.000	0.000	0.000	0.000	0.000	0.000	0.000	0.000	0.000	0.000
0.000	0.000	0.000	0.000	0.000	0.000	0.000	0.000	0.000	0.000
0.000	0.000	0.000	0.000	0.000	0.000	0.000	0.000	0.000	0.000
0.000	0.000	0.000	0.000	0.000	0.000	0.000	0.000	0.000	0.000
0.000	0.000	0.000	0.000	0.000	0.000	0.000	0.000	0.000	0.000
0.000	0.000	0.000	0.000	0.000	0.000	0.000	0.000	0.000	0.000

UBINF=0.2350
EGMEAN= 0.0187
BSIZE= 0.0035
GRATE= 0.000272
VELFACT= 0.2150
SPA POS1= 4 10
SPA POS2= 4 11

(b) ↑Tank Base

Fig 5 : Local gas hold-up distribution via square cells network Model for U_t = 0.235 m/s

assumed.

The simulation agrees qualitatively with Pic 1. For example, both Pic.1 and Fig.5(a) show that there are no air bubbles toward the middle of the lower vessel. The simulated map also shows that the local gas hold-up distribution is predicted to decrease towards the vessel wall. In accordance to this, Pic.1 indeed shows that less air bubbles are found in the wall region. In the lower half of the vessel, the predicted result represents more of the actual case. The uniform bubble size assumption means that most of the air bubbles possess velocities that are greater than the radial and axial water velocity. The buoyancy force in each bubble helps it flow upwards into the next row of cells, toward the liquid surface.

One of the shortcomings about the model is its inability to incorporate the strong water radial force flowing out of the impeller. This could be due to the liquid velocity strength which is under predicted by the model. From Fig.5(a) and Fig.5(b), the model predicts that the highest local hold-ups are in the cells where the gas is sparged in, at cells I=4,J=10 and I=4,J=11. But, Pic.1 shows that the air is swept to the right towards the vessel wall by the water flowing out of the impeller. Therefore, the model should predict a high hold-up in I=5 and I=6 instead.

Fig.5(a) shows that in the upper half of the vessel, the local gas hold-ups decline rapidly as the radial outflow approaches the vessel wall. This is partly because there is upward co-current flow of gas and liquid in this region, and also partly because only a small proportion of the gas leaving the impeller is actually predicted to be dispersed as far as the wall.

In contrast to Pic 1, Fig 5.(a) shows that the gas hold-up is low in the downward liquid flow near the shaft of the impeller. Pic.1 shows that the bubbles are small in this part of the vessel. Since one of the assumptions is uniform bubble size distribution, the model does not take into account the downward water flow that could suppress the smaller and slower bubbles. Hence, it predicts that most of the air bubbles of uniform size flow upwards and do not recirculate towards the impeller.

Fig.6(a) and 6(b) show the simulated results when the bubble rise velocity is reduced by 40% to u_t= 1.35 m/s which means the bubbles sizes are assumed to be in the smaller range. The predicted overall gas hold-up, $\bar{\varepsilon}_g$, is 3.25% which is now closer to the experimental value of 3.81%. The local gas hold-up distribution still shows the

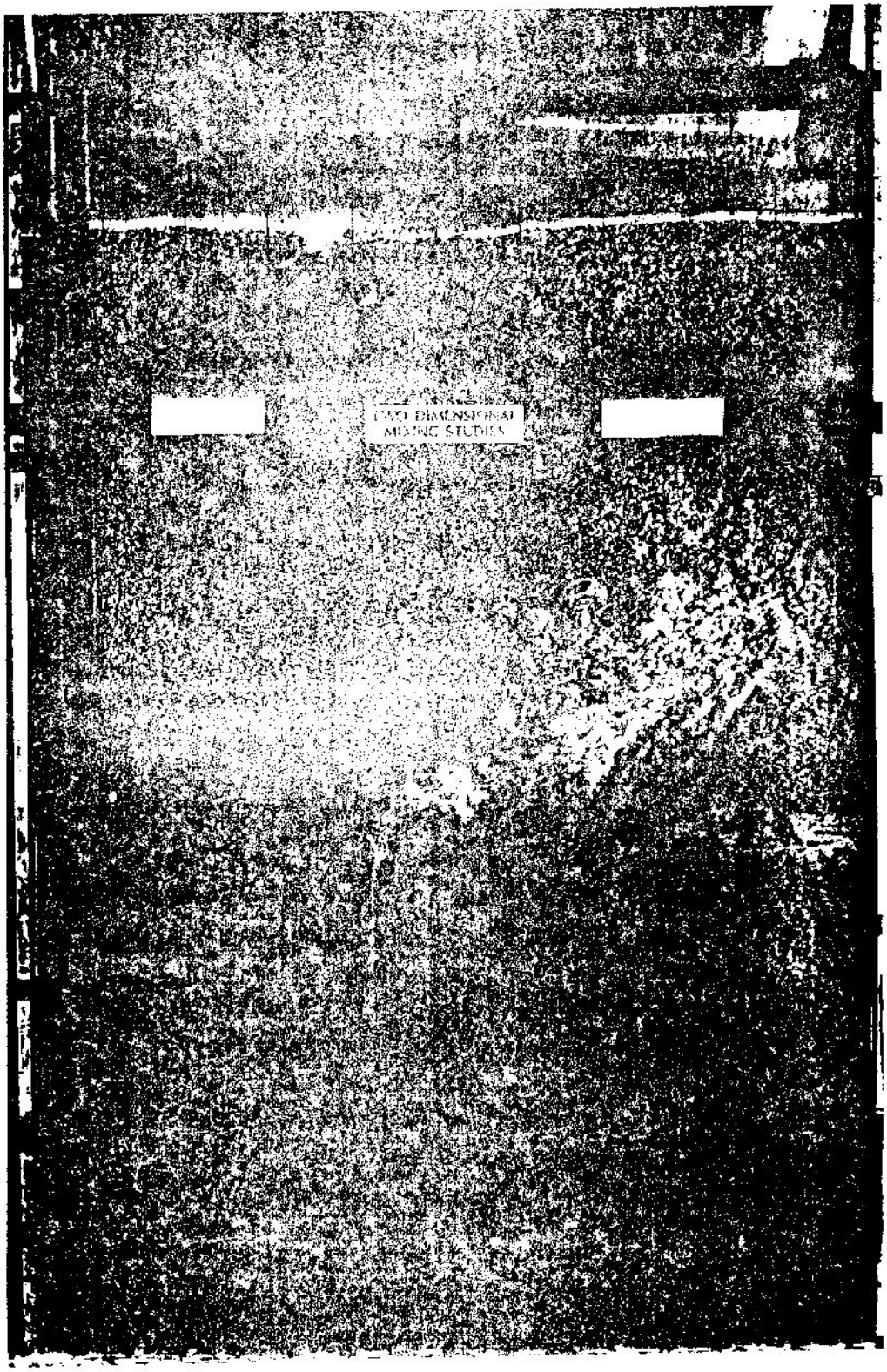

Pic 1 Q_L=12.0 x 10^{-6} m^3/s, Q_G=2.72 x 10^{-4} m^3/s

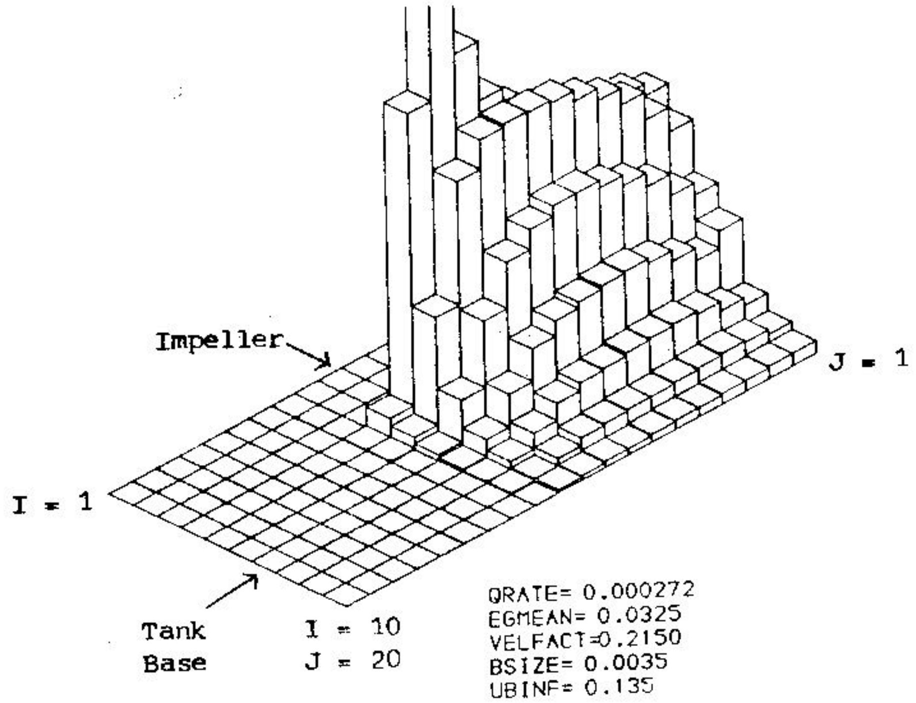

(a)

I = 1, J = 1 (top left); I = 10 (top right); J = 20 (bottom left); Impeller → (row 11); ↑ Tank Base (right column)

0.042	0.065	0.102	0.131	0.115	0.081	0.065	0.024	0.013	0.008
0.014	0.047	0.088	0.139	0.131	0.089	0.054	0.029	0.016	0.008
0.007	0.020	0.066	0.143	0.149	0.103	0.062	0.035	0.017	0.007
0.005	0.014	0.048	0.142	0.160	0.112	0.069	0.037	0.016	0.007
0.003	0.010	0.040	0.149	0.168	0.119	0.072	0.036	0.015	0.006
0.001	0.006	0.030	0.159	0.175	0.124	0.071	0.035	0.014	0.006
0.000	0.002	0.017	0.172	0.177	0.124	0.069	0.033	0.014	0.005
0.000	0.000	0.000	0.186	0.178	0.117	0.065	0.032	0.013	0.004
0.000	0.000	0.000	0.224	0.176	0.104	0.055	0.027	0.012	0.004
0.000	0.000	0.000	0.316	0.157	0.074	0.034	0.016	0.007	0.003
0.000	0.000	0.000	0.202	0.077	0.031	0.013	0.006	0.002	0.002
0.000	0.000	0.000	0.013	0.008	0.004	0.002	0.001	0.001	0.000
0.000	0.000	0.000	0.001	0.001	0.000	0.000	0.000	0.000	0.000
0.000	0.000	0.000	0.000	0.000	0.000	0.000	0.000	0.000	0.000
0.000	0.000	0.000	0.000	0.000	0.000	0.000	0.000	0.000	0.000
0.000	0.000	0.000	0.000	0.000	0.000	0.000	0.000	0.000	0.000
0.000	0.000	0.000	0.000	0.000	0.000	0.000	0.000	0.000	0.000
0.000	0.000	0.000	0.000	0.000	0.000	0.000	0.000	0.000	0.000
0.000	0.000	0.000	0.000	0.000	0.000	0.000	0.000	0.000	0.000
0.000	0.000	0.000	0.000	0.000	0.000	0.000	0.000	0.000	0.000

UBINF=0.1350
EGMEAN= 0.0325
BSIZE= 0.0035
QRATE= 0.000272
VELFACT= 0.2150
SPA POS1= 4 10
SPA POS2= 4 11

(b)

Fig 6: Local Gas Hold-up Distribution For U_t = 0.135 m/s

same trend but the values have become higher in all cells. Fig.6(a) also shows a more distinctive gas hold-up than Fig.5(a) in the region near the wall confirming the presence of smaller bubbles. Interestingly, Fig.6(a) and (b) start to indicate the effect of gas coalescence by showing that gas hold-ups are no longer concentrated in column I=4 only, but also in columns I=5 and I=6. Pic.1 shows that bigger bubbles are found in the fresh air path. The bigger bubbles actually consist of millions of smaller bubbles which is why the model is now able to predict better gas hold-up values for this region.

Fig.7(a) and 7(b) simulate the conditions for Pic.1 at a very low bubble rise velocity of 0.035m/s. The whole upper half of the vessel indicates tracers of air bubbles. About three-quarter of the lower vessel including the tank base display some gas hold-ups although they are mostly concentrated near the wall or at cell I=10.

With the exception of the predicted results calculated for the lower vessel, the simulation in Fig.7(a) is the closest to the experimental situation in Pic.1. The region near the impeller shaft shows distinctive local gas hold-ups at columns I=1,2,3. This indicates that in this region the bubbles are small and so, they possess slower bubble rise velocity. Fig. 7(a) also exhibits that gas hold-ups decrease towards the vessel wall. Near the impeller region but at midway position of the vessel or columns I=4,5,6,7,8,9,10 and row J=10 the map displays a slight indication of bubbles coalescence, because of the decreasing hold-ups along the I columns. More importantly Fig.7(a) shows that this model has a very high potential to represent the real situation if only it can incorporate the bubble size distribution.

6.0 Conclusion

The simple zones-in-loops model is inadequate to predict the gas and liquid flow behaviour in a stirred vessel. because of the simple downward and upward water flow assumption.

The square-cells-network model is more superior than the simple model. It predicts a more comprehensive water flow structure by incorporating the liquid lateral exchanges and the radial flows. The lateral flows between adjacent cells is an important measure for describing the mixing of gas and liquid in the vessel. The model has a potential to simulate the flow behaviour more realistically if only it undertakes the different bubble sizes in formulating the model.

It should be emphasized that once the gas and liquid

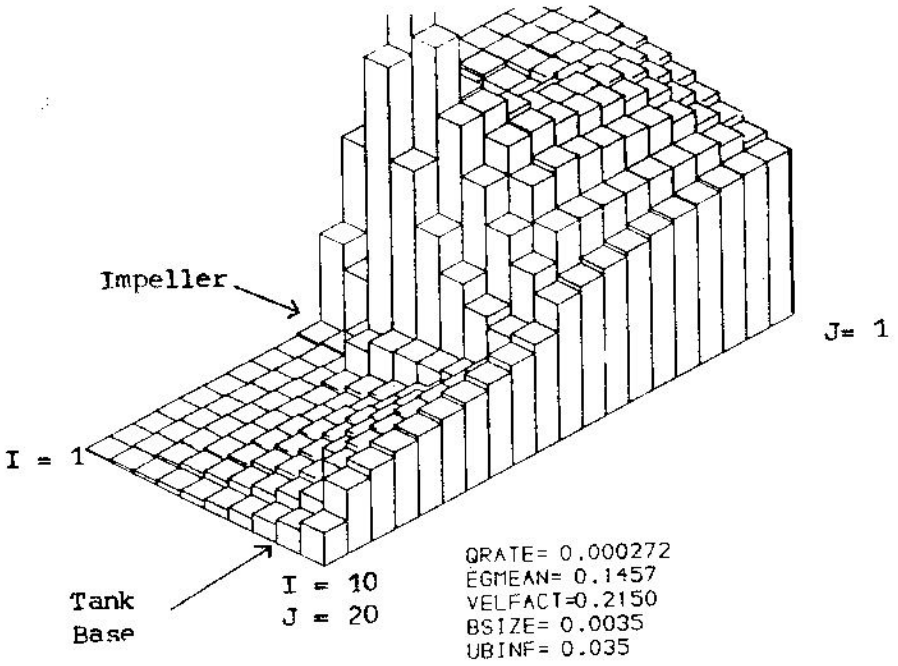

(a)

I = 1
J = 1

I = 10

0.257	0.257	0.255	0.252	0.246	0.238	0.227	0.217	0.207	0.199
0.258	0.259	0.260	0.260	0.259	0.254	0.243	0.231	0.219	0.199
0.258	0.260	0.262	0.264	0.269	0.271	0.263	0.249	0.224	0.197
0.258	0.259	0.259	0.262	0.270	0.281	0.276	0.258	0.224	0.193
0.258	0.257	0.252	0.252	0.266	0.286	0.284	0.261	0.224	0.190
0.257	0.253	0.241	0.240	0.260	0.288	0.289	0.264	0.223	0.186
0.253	0.243	0.216	0.221	0.266	0.295	0.295	0.267	0.223	0.181
0.243	0.213	0.130	0.222	0.286	0.309	0.302	0.271	0.223	0.176
0.217	0.139	0.107	0.280	0.331	0.327	0.299	0.264	0.222	0.170
0.113	0.083	0.038	0.506	0.406	0.326	0.265	0.219	0.186	0.164
0.008	0.011	0.038	0.384	0.273	0.206	0.163	0.137	0.125	0.131
0.005	0.008	0.010	0.055	0.068	0.070	0.071	0.075	0.090	0.121
0.005	0.008	0.011	0.021	0.029	0.036	0.047	0.064	0.089	0.113
0.005	0.008	0.012	0.017	0.023	0.032	0.047	0.067	0.088	0.106
0.004	0.007	0.012	0.018	0.023	0.035	0.049	0.066	0.086	0.101
0.004	0.007	0.012	0.018	0.025	0.035	0.045	0.063	0.082	0.096
0.004	0.007	0.012	0.017	0.024	0.032	0.040	0.057	0.078	0.092
0.005	0.007	0.011	0.016	0.021	0.028	0.035	0.044	0.071	0.086
0.005	0.006	0.009	0.013	0.017	0.022	0.028	0.037	0.048	0.077
0.005	0.004	0.007	0.007	0.009	0.012	0.014	0.02	0.029	0.040

UBINF=0.0350
EGMEAN= 0.1457
BSIZE= 0.0035
QRATE= 0.000272
VELFACT= 0.2150
SPA POS1= 4 10
SPA POS2= 4 11

Impeller

J = 20

Tank Base

(b)

Fig 7 : Local Gas Hold-up Distribution for U_t = 0.035 m/s

behaviour is properly described, other important properties will follow directly. For instance, the gas-liquid mixing rates will be predictable. The liquid phase mixing characteristics and the gas phase RTD can both be independently predicted. In addition, the surface areas and local mass transfer coefficients will be obtained implicitly. Most important of all these will be a proper basis for the rational calculations of gas-liquid behaviour soundly based in the pyhsical realities of the gas-liquid flow.

7.0 Reference

a. Cooper,R.G., and Wolf,D.,1968,Can. J. Chem Eng.46,94
b. Hackett.L.A.,1985 Ph.D Thesis,U.M.I.S.T
c. Mann,R.,Mavros,P.P, and Middleton,J.C.,1981,I.Chem Eng Series,64,G1
d. Mann,R. and Hackett,L.A.,1988,Proc 6th Euro . Conf.Mixing(BHRA Fluid Engineering, Cranfield),321
e. Saidina Amin,N.A.,1988,M.Sc Diss.U.M.I.S.T.

8.0 Nomenclature

Unaerated dynamic liquid height	H_L
Aerated dynamic liquid height	H_O
Bubble rise velocity	u_t
Superficial gas velocity	u_G
superficial liquid velocity	u_L
Local gas hold-up	ε_i
Average gas hold-up	$\bar{\varepsilon}_G$

Computer Terminology	
Volumetric gas input rate,m^3/s	QRATE
Average gas hold-up	EGMEAN
Velocity factor	VELOCITY FACTOR
Bubble rise velocity	UBINF
Sparger position 1	SPA POS1
Sparger position 2	SPA POS2
Bubble size	BSIZE